Influence of Excision of a Methylene Group from Glu-376 (Glu376→Asp Mutation) in the Medium Chain Acyl-CoA Dehydrogenase-Catalyzed Reaction†

Kevin L. Peterson, David S. Galitz, and D. K. Srivastava*

Biochemistry Department, North Dakota State University, Fargo, North Dakota 58105

Received October 20, 1997; Revised Manuscript Received December 2, 1997

ABSTRACT: The human liver medium chain acyl-CoA dehydrogenase (MCAD)-catalyzed reaction proceeds via abstraction of an α-proton from the acyl-CoA substrates by the carboxyl group of Glu-376. By using the methods of site-directed mutagenesis, we replaced Glu-376 by Asp (E376D mutation), expressed the wild-type and mutant enzymes in *Escherichia coli*, purified them to homogeneity, and compared their kinetic properties. The steady-state kinetic data revealed that the E376D mutation impaired (by about 15−20-fold) the turnover rate of the enzyme as well as its inactivation by 2-octynoyl-CoA. There was no selective solvent deuterium isotope effect on enzyme catalysis. These results lead to the suggestion that the carboxyl group of Asp-376 does not serve as efficient catalytic base as the carboxyl group of Glu-376. The E376D mutation impaired the octanoyl-CoA-dependent reductive half-reaction such that the rate-limiting step of enzyme catalysis shifted from the product dissociation step (in the case of the wild-type enzyme) to the flavin reduction step, and abolished the previously noted kinetic and thermodynamic correspondences between the octanoyl-CoA-dependent reductive half-reaction and the enzyme−octenoyl-CoA interaction [Kumar, N. R., and Srivastava, D. K. (1994) *Biochemistry* 33, 8833−8841]. Arguments are presented that the Glu-376→Asp mutation results in uncoupling between the proton transfer and protein conformational change steps during enzyme catalysis.

Due to the availability of efficient expression systems for human liver medium chain acyl-CoA dehydrogenase (MCAD),[1] ease in purification of the enzyme, and the possibility of creating site-specific mutations, we and others have been encouraged to utilize human liver enzyme toward mechanistic and/or structural−functional goals (*1*−*5*). Such studies have been further facilitated by a high degree of sequence homology among MCADs of different biological origins (*6*), and high-resolution X-ray crystallographic structures of pig liver and human liver enzymes (*2, 7*). However, despite the fact that a number of site-specific mutants of human liver MCAD have been created in recent years in different laboratories, detailed structural−functional and mechanistic studies involving the purified preparations of the wild-type and mutant enzymes have been sparse (*4, 8*−*9*).

It has been known that the MCAD-catalyzed reaction proceeds via abstraction of the α (*pro-R*)-proton from acyl-CoA substrates by the active site base Glu-376, followed by transfer of the *β*-hydrogen in the form of a hydride to the N-5 position of the isoalloxazine ring of FAD (*6, 10*) (eq 1).

The functional role of Glu376 during enzyme catalysis was originally inferred on the basis of inactivation of the enzyme (via covalent modification of the carboxyl group of Glu376) by 2-octynoyl-CoA as a mechanism-based inactivator. However, the latter reaction was envisaged to proceed via abstraction of the *γ*-proton of 2-octynoyl-CoA (since the latter compound is devoid of the α-protons) by the same active site base Glu-376 (*11*).

Figure 1 shows the spatial relationship among the enzyme-bound FAD, octenoyl/octanoyl-CoA (C_8−CoA), and the Glu-376 residue at the active site of the enzyme. One of the oxygen atoms (viz., OE2) of the Glu-376 carboxyl group is oriented to abstract the *pro-R* α-hydrogen of C_8−CoA as a proton, and the N5 nitrogen on the *re*-face of the isoalloxazine ring of FAD is oriented to accept the *pro-R β*-hydrogen (from C_8−CoA) as a hydride anion (*10*). Based on the distance measurements between the carboxyl oxygens of Glu-376 and different carbons of C_8−CoA (*5*), it appears likely that the same oxygen atom (viz., OE2) which abstracts the α-proton from octanoyl-CoA substrate also abstracts the *γ*-proton from 2-octynoyl-CoA during the course of covalent modification and inactivation of the enzyme.

We previously demonstrated that the rate-limiting step of the enzyme, utilizing octanoyl-CoA as a physiological

† This work was supported by grants from the National Science Foundation (MCB-9507292) and the American Heart Association (AHA-96008200).

* To whom correspondence should be addressed.

[1] Abbreviations: MCAD, medium chain acyl-CoA dehydrogenase; FAD, flavin adenine dinucleotide; OceCoA, 2-octenoyl coenzyme A; IPCoA, 3-indolepropionyl coenzyme A; IACoA, *trans*-3-indoleacryloyl coenzyme A; $FcPF_6$, ferricenium hexafluorophosphate; ETF, electron-transferring flavoprotein; CT, charge-transfer; EDTA, ethylenediaminetetraacetic acid.

S0006-2960(97)02590-7 CCC: $15.00
Published on Web 01/23/1998

substrate, was the dissociation "off-rate" of the reaction product, octenoyl-CoA, from the oxidized enzyme site (*12*−*14*). We further observed that the binding of octenoyl-CoA to the oxidized form of the enzyme was kinetically as well as thermodynamically equivalent to the reduction of the oxidized enzyme by octanoyl-CoA (*5*, *15*). For example, the equilibrium constant (K_{eq}) for the E−FAD + octanoyl-CoA ⇌ E−$FADH_2$−octenoyl-CoA reaction (155 nM) was found to be identical to the dissociation constant for the binding of octenoyl-CoA to E−FAD (153 nM), i.e., E−FAD + octenoyl-CoA ⇌ E−FAD−octenoyl-CoA (*5*). Besides, both these reactions conformed to the biphasic kinetics, with fast ($1/\tau_{fast}$) and slow ($1/\tau_{slow}$) relaxation rate constants of the former (chemical transformation) reaction of 435 and 44.2 s^{-1}, respectively, and for the latter (physical interaction) process of 482 and 53.4 s^{-1}, respectively (5; eq 2).

$$\text{E}-\text{FAD} + \text{OcaCoA} \rightleftharpoons \text{E}-\text{FAD}-\text{OcaCoA} \rightleftharpoons (\text{E}-\text{FADH}_2-\text{OceCoA})^* \rightleftharpoons (\text{E}-\text{FADH}_2-\text{OceCoA})^{**}$$

$$K_{eq} = \frac{[\text{E}-\text{FAD}][\text{OcaCoA}]}{[(\text{E}-\text{FADH}_2-\text{OceCoA})^*] + [(\text{E}-\text{FADH}_2-\text{OceCoA})^{**}]} = 155\ \text{nM}$$

$$1/\tau_{fast} = 435\ s^{-1},\ 1/\tau_{slow} = 44.2\ s^{-1}$$

$$\text{E}-\text{FAD} + \text{OceCoA} \rightleftharpoons \text{E}-\text{FAD}-\text{OceCoA} \rightleftharpoons (\text{E}-\text{FAD}-\text{OceCoA})^* \rightleftharpoons (\text{E}-\text{FAD}-\text{OceCoA})^{**}$$

$$K_d = \frac{[\text{E}-\text{FAD}][\text{OceCoA}]}{[(\text{E}-\text{FAD}-\text{OceCoA})^*] + [(\text{E}-\text{FAD}-\text{OceCoA})^{**}]} = 153\ \text{nM}$$

$$1/\tau_{fast} = 482\ s^{-1},\ 1/\tau_{slow} = 53.4\ s^{-1} \qquad (2)$$

The species denoted by single and double asterisks represent the isomerized forms of the respective complexes. It should be noted that the major difference between the two reactions of eq 2 is that the former accompanies "chemistry" whereas the latter simply involves changes in the electronic structures of the enzyme-bound FAD and octenoyl-CoA species. A qualitatively similar conclusion was drawn for the binding of 2-octynoyl-CoA to the enzyme site (*5*). In light of these observations, we proposed that all the above (functionally diverse) processes, involving different C_8-CoAs, were dictated by obligatory changes in the protein conformation (*5*, *15*−*16*). According to this hypothesis, the rate of proton and/or hydride transfer during the octanoyl-CoA-dependent reductive half-reaction of the enzyme must be equal to or greater than the rate of the protein conformational changes. The question arose whether the above processes were somehow linked together during the reductive half-reaction of the enzyme. To probe this, we considered impairment of the rate of proton transfer by replacing the enzyme's active site residue Glu376 by Asp (via site-directed mutagenesis), and compared the kinetics of the enzyme catalysis and enzyme−ligand interaction.

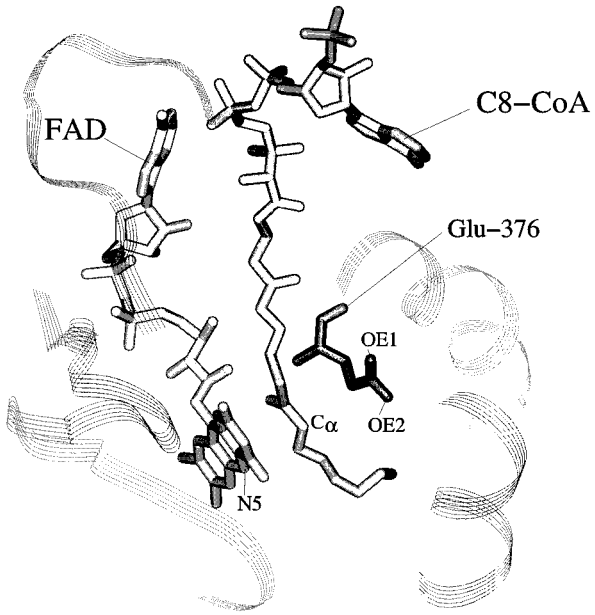

FIGURE 1: Spatial relationship of FAD, C_8−CoA, and Glu-376 within the active site of pig liver medium chain acyl-CoA dehydrogenase. The two oxygen atoms of the carboxyl group of Glu-376, namely, OE1 and OE2, are labeled. The broken ribbons are displayed to show the boundary of the active site region of the enzyme. This structure was created on the Silicongraphics(O_2) molecular modeling station with the help of the software Insight II.

Knowles and his collaborators (*17*) postulated that the "void" created by excision of a methylene group from the side chain chain of Glu165 (Glu165→Asp mutation) in the case of triosephosphate isomerase could be occupied by a water molecule, and the latter might serve as a proton shuttle between the carboxyl group of Asp165 and *pro-R* hydrogen of dihydroxyacetone phosphate. Although such a possibility was negated by their experimental findings (*17*), as well as in enzymes where the carboxyl group of Glu served as the active site base, and Glu was replaced by Asp via site-directed mutagenesis (*18*−*19*), such a possibility during the MCAD-catalyzed reaction could not be, apriorily, ruled out. This was an added consideration for comparing the kinetics of the wild-type and Glu376 → Asp mutant enzyme catalyzed reactions. Via these experiments, we hoped to distinguish whether the carboxyl group of Asp-376 served as a "specific" or "general" base catalyst during the E376D mutant enzyme-catalyzed reaction. It should be pointed out that prior to this investigation, Ghisla et al. (*9*) casually mentioned that the turnover rate of the Glu376→Asp mutant enzyme was about 10% of the wild-type enzyme.

MATERIALS AND METHODS

Materials. Octanoyl-CoA, EDTA, deuterium oxide, and deuterium chloride were purchased from Sigma. 2-Octynoic acid and ferricenium hexafluorophosphate ($FcPF_6$) were purchased from Aldrich. *trans*-2-Octenoic acid was from Pfaltz and Bauer. The DH5α and TG1 *E. coli* cells were purchased from Gibco/BRL and Strategene, respectively. The primers used for PCR reactions and DNA sequencing were synthesized by Integrated DNA Technology (Coralville, IA). The T7 promoter and terminator sequences were purchased from Novagen. T4 DNA ligase and NZ-amine growth medium were purchased from Promega and Sheffield

products, respectively. All other reagents were of analytical grade.

Methods. We performed all experiments, unless otherwise noted, in the standard buffer of 50 mM potassium phosphate (K_2HPO_4), pH 7.6, containing 0.3 mM EDTA, 10% glycerol, and 100 mM KCl.

We synthesized *trans*-2-octenoyl-CoA (OceCoA) and 2-octynoyl-CoA (OcyCoA) using the mixed anhydride method of Bernert and Sprecher (*20*). The molar extinction coefficients of OcyCoA and OceCoA were taken to be 20.9 and 20.4 mM^{-1} cm^{-1} at 260 and 258 nm, respectively (*5*, *21*). The extinction coefficients for octanoyl-CoA (OcaCoA) and acetoacetyl-CoA (AcAcCoA) were taken to be 15.6 mM^{-1} cm^{-1} at 259 nm. The molar extinction coefficient of ferricenium hexafluorophosphate ($FcPF_6$) was taken to be 0.41 mM^{-1} cm^{-1} at 617 nm, or 4.3 mM^{-1} cm^{-1} at 300 nm (*22*). For IPCoA and IACoA, the molar extinction coefficients were taken to be 18.2 and 26.5 mM^{-1} cm^{-1} at 259 and 367 nm, respectively (*23*). The molar extinction coefficients for the wild-type and E376D mutant enzymes were taken to be 15.4 mM^{-1} cm^{-1} at 446 nm (*24*). Although Glu376→Asp mutation resulted in a small perturbation in the FAD spectrum (our unpublished results), both wild-type and mutant enzyme showed an isosbestic point at 446 nm. Hence, the molar extinction coefficient of the mutant enzyme was taken to be the same as that of the wild-type enzyme.

Creation of the Glu376→Asp (E376D) Mutant. The pET11a-HMCAD plasmid (*25*) was utilized to create the E376D mutation through oligonucleotide-directed mutagenesis (*26*). This method involved the formation of two primary PCR products, designated as PCR1 and PCR2, by utilizing two complementary internal primer sequences containing the mutation site. The PCR1 reaction utilized a 27-mer mutant primer (5′TTGTGAAGTACC*ATC*ATAAATCTGATA3′), containing the reverse complement of the mutation site and the T7 promoter (5′TAATACGACTCACTATAGGGGAATTGT3′). A reaction mixture containing 1.37 pmol of pET11a-HMCAD, 2 μM T7 promoter primer, 1 μM internal primer, 0.2 mM dNTP, 1× native pfu buffer, and 2.5 units of native pfu (in a total volume of 50 μL) was subjected to a 20 hot-start PCR cycle (*38*) at 80 °C on a Minicycler thermal controller (MJ Research). The above cycles involved denaturation (94 °C, 30 s), annealing (52 °C, 30 s), and extension (72 °C, 2 min). The extension time of the last cycle was maintained for 15 min to ensure the completion of the reaction. This reaction produced a 1.2 kb oligonucleotide fragment. An identical reaction condition was adopted to synthesize the PCR2 product. The latter protocol involved a 27-mer mutant oligonucleotide (5′TATCAGATTTAT*GAT*GGTACTTCACAA3′), containing the normal complement of the mutation site and the T7 terminator (5′GCTAGTTATTGCTCAGCGGTG3′). The PCR2 reaction produced a 0.8 kb fragment.

Both the PCR products were separated by agarose gel electrophoresis, and purified by the electroelution procedure of Moore (*27*). The third PCR reaction was performed by using PCR products 1 and 2 as a mixed template and T7 promoter and T7 terminator as external primers. The reaction conditions for the last PCR reaction involved 63 of ng PCR 1 product, 38 ng of PCR 2 product, 2 μM each external primer, 0.2 mM dNTP, 1× native pfu buffer, and 2.5 units of native pfu in a total volume of 50 μL. The PCR3 reaction was hot-started at 80 °C, for 20 cycles of denaturation (94 °C, 30 s), annealing (45 °C, 30 s for the first cycle, 48 °C, 30 s for the remaining cycles), and extension (72 °C, 3 min). The final extension cycle was maintained for 15 min to ensure the completion of the reaction. The PCR3 reaction yielded a 2 kb oligonucleotide fragment, which was ligated at the *Xba*I and *Bam*HI sites into the pBluescript II (KS-) plasmid, and the resultant plasmid was propagated in the DH5α cells, using the standard molecular biology procedures as outlined by Sambrook et al. (*28*). The plasmids containing the mutated MCAD sequence were identified by blue/white screening on LB agar plates, containing 100 μg/mL ampicillin and 50 μg/mL X-gal. The mutant plasmid was subjected to sequencing at the DNA sequencing facility of University of Chicago, Cancer Research Center. Since the MCAD gene (PCR3) contained an extra 800 bp sequence following the stop codon, the sequencing was performed using the internal primer, 5′TTCTGGAGCTGAAACAGTGGC3′, 39 bp downstream from TAA.

The E376D mutant sequence was restriction-digested out of pBluescript II (KS-) with *Xba*I and *Hin*dIII, purified by agarose gel electrophoresis, and then ligated at *Xba*I/*Hin*dIII sites in the expression plasmid pTrc 99B (obtained as a gift from Drs. Andreas Nandy and Sandro Ghisla). The resultant plasmid was transformed into the DH5α cells and propagated. The mutant enzyme was expressed in the *E. coli* TG1 cells essentially as described by Nandy et al. (*3*), except for the substitution of the dYT medium by the NZ-amine medium (*5*). The pTrc-MCAD (wild-type) plasmid was obtained as gift from Drs. Andrea Nandy and Sandro Ghisla. Both wild-type and E376D mutant enzymes were purified by our previously developed protocol (*5*). The latter expression system increased the total yield of the wild-type and mutant enzymes by about 3-fold as compared to our recently optimized growth and expression conditions (*29*). The final preparations of both wild-type and mutant enzymes were subjected to the de-greening procedure (to remove the contaminant CoA persulfide) as described by Nandy et al. (*3*).

The SDS−PAGE electrophoresis was performed according to the procedure of Weber and Osborn (*30*).

Steady-State Kinetic Experiments. The steady-state kinetic experiments were performed on a Perkin-Elmer lambda 3B spectrophotometer, equipped with the thermostated cell holder and magnetic stirrer. The initial rates of the IPCoA- and octanoyl-CoA-dependent reactions were measured by monitoring the formation of IACoA at 367 nm ($\epsilon_{367} = 26.5$ mM^{-1} cm^{-1}) and reduction of ferricenium hexafluorophosphate ($FcPF_6$) at 300 nm ($\epsilon_{300} = 4.3$ mM^{-1} cm^{-1}), respectively.

The kinetics of inactivation of the enzyme by 2-octynoyl-CoA were determined by incubating both wild-type and mutant enzymes with 2-octynoyl-CoA under pseudo-first-order conditions ([2-octynoyl-CoA] ≫ [enzyme]) in a thermostated water bath at 25 °C. A 10 μL aliquot of the reaction mixture was withdrawn at different time intervals and was directly transferred to the enzyme assay mixture, containing 100 μM IPCoA and 250 μM $FcPF_6$. The initial rate of enzyme catalysis was measured by following the increase in absorbance at 367 nm as outlined above. The time-dependent decrease in activity was analyzed according to the single-exponential rate equation by Grafit 3.0 (Erithacus Software).

For the deuterium isotope experiments, both enzymes and substrates were first lyophilized, and the resultant powder was dissolved in the standard phosphate buffer prepared in D_2O and the pH adjusted by DCl to a (pD) value of 7.2, which was taken to be equal to the pH of 7.6 (*39*). For the deuterium isotope experiments, the stock solution of $FcPF_6$ was prepared by dissolving the crystals in 10 mM DCl.

Transient Kinetic Experiments. The single-wavelength transient kinetic experiments were performed on an Applied Photophysics SX-17 MV stopped-flow system (optical path length 10 mm, dead time 1.3−1.5 ms). Depending on the type of the experiment, the stopped-flow was configured in either a single or a sequential mixing mode. In the single mixing mode the contents of both syringes were diluted by 50%, whereas in the sequential mixing mode the contents of syringes A ad B were diluted by 75% and the content of syringe C was diluted by 50%. The stopped-flow kinetic traces were analyzed by the data analysis package provided by Applied Photophysics. Detailed experimental protocols for determining the reductive half-reaction, oxidative half-reaction, dissociation off-rate constant of octenoyl-CoA from the oxidized enzyme sites, and kinetics of interaction of octenoyl-CoA to the oxidized enzyme site have been elaborated by Kumar and Srivastava (*15, 16*), Peterson et al. (*5*), and Peterson and Srivastava (*29*).

RESULTS

The Glu-376 to Asp (E376D) mutation in the coding sequence of the human liver MCAD gene was confirmed by DNA sequence analysis (see Materials and Methods). The sequencing data revealed that adenine at position 1131 was replaced by thymine, leading to the change in the Glu-376 codon from GAA to the Asp-376 codon GAT. Besides this, no other change in the nucleotide base from 611 to 1194 was discerned from the sequencing data. The level of expression as well as the purification pattern of the mutant enzyme was identical with those of the wild-type enzyme. The purified preparations of both these enzymes showed a single band on SDS gel electrophoresis (*30*), and their A_{280}/A_{450} ratio was in the range of 5.0−5.1 (*24*).

One of the interesting features of the enzyme(s) purified by using the current expression system (see Materials and Methods) was its greenish color, which was characterized by its absorption maximum at 710 nm. This was presumably due to the contamination of CoA-persulfide in the enzyme preparation (*31*). Such a property of the enzyme was also noted by Nandy et al. (*3*). To our surprise, the green color was more pronounced in the case of the wild-type enzyme than the E376D mutant enzyme. No such green color was detected (or at least it was miniscule) when we purified the enzyme using our previous expression system and growth conditions (*5*). These observations are inconsistent with the explanation that the green color is absent in the wild-type MCAD preparation due to the presence of two negatively charged residues (Glu-99 and Glu-376) at the active site of the enzyme (*32*). However, irrespective of the origin of the green color in the enzyme preparations, we subjected them to the sodium dithionite treatment, followed by a quick gel filtration on a Sephadex G-25 column, as described by Nandy et al. (*3*).

Steady-State Kinetics of the Enzyme. We performed the steady-state kinetic experiments of the wild-type and the E376D mutant enzymes, utilizing indolepropionyl-CoA (IPCoA) as a chromogenic substrate (*23, 33*−*36*) and octanoyl-CoA as a physiological substrate (*5, 15, 16*), and saturating concentrations of ferricenium hexafluorophosphate ($FcPF_6$) as an electron acceptor. A comparative account of the steady-state kinetic parameters of these enzymes is given in Table 1. Note that the E376D mutation results in a decrease in the k_{cat} values of both IPCoA- and octanoyl-CoA-dependent reactions by about 20-fold. On the other hand, whereas the E376D mutation does not influence the apparent K_m for IPCoA, it increases the K_m for octanoyl-CoA by a factor of 3. We believe the above variation in the K_m is due to the complexity of the microscopic pathways of the IPCoA- and octanoyl-CoA-dependent reactions (*15, 16, 34, 35*).

Table 1: Steady-State Kinetic Parameters and Solvent Deuterium Isotope Effects on the Wild-Type and E376D MCAD-Catalyzed Reactions[a]

		IPCoA[b]		OcaCoA[c]	
enzyme	solvent	K_m (μM)	k_{cat} (S^{-1})	K_m (μM)	k_{cat} (S^{-1})
wild-type	H_2O	8.7 ± 0.3	3.4 ± 0.03	2.6 ± 0.4	15.6 ± 0.5
wild-type	D_2O	2.8 ± 0.4	1.96 ± 0.1	5.6 ± 0.6	10.6 ± 0.4
E376D	H_2O	9.0 ± 0.9	0.17 ± 0.01	8.7 ± 0.6	0.75 ± 0.08
E376D	D_2O	3.34 ± 0.6	0.08 ± 0.01	2.6 ± 0.5	0.40 ± 0.02

[a] IPCoA and OcaCoA refer to 3-indolepropionyl-CoA and octanoyl-CoA, respectively. [b] Determined in the presence of 250 mM $FcPF_6$. [c] Determined in the presence of 350 mM $FcPF_6$.

To examine the influence of a potential active site water molecule serving as a proton shuttle (see the introduction), we investigated the solvent deuterium isotope effect on the steady-state kinetic parameters of the wild-type and the E376D mutant enzymes (Table 1). As can be seen from the data of Table 1, both K_m and k_{cat} values of the wild-type and mutant enzymes are affected upon substitution of solvent H_2O by D_2O. For example, the K_m for IPCoA is decreased by about 3-fold (upon substitution of H_2O by D_2O) involving both wild-type and mutant enzymes. On the contrary, whereas the K_m for octanoyl-CoA is increased by 2-fold (under the above condition) in the case of the wild-type enzyme, it is decreased by 3-fold in the case of the mutant enzyme. It is interesting to note that regardless of the substrate or the enzyme type, H_2O to D_2O substitution impairs the turnover rate of the enzyme by 1.5−2.0-fold. However, the latter effects are not so great, particularly in light of the view that solvent deuterium, besides providing the general medium effect, has the potential to influence the ionization states of the enzyme site groups as well as the protein conformation (see Discussion).

Inactivation of Wild-Type and E376D Mutant Enzymes by 2-Octynoyl-CoA. Given that the mechanistic pathway of the 2-octynoyl-CoA-dependent inactivation of the enzyme is similar to the octanoyl-CoA-dependent reductive half-reaction (see the introduction), we investigated the influence of the E376D mutation on the kinetics of inactivation of the enzyme by 2-octynoyl-CoA. We compared the time-dependent loss in enzyme activity upon incubation of both wild-type and mutant enzymes with 2-octynoyl-CoA under pseudo-first-order conditions ([2-octynoyl-CoA] ≫ [enzyme]). The solid, smooth lines are the best fit of the data for a single exponential decrease in the enzyme activity with the rate constants of 0.031 ± 0.0002 and 0.002 ± 0.0002 s^{-1} for the wild-type and mutant enzymes, respectively.

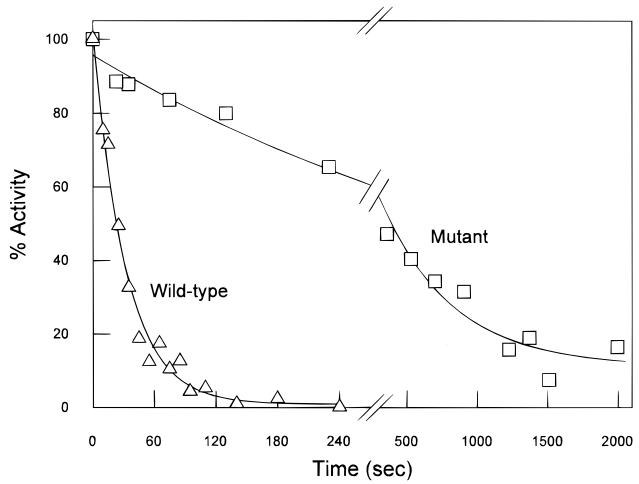

FIGURE 2: Inactivation of the wild-type and E376D mutant MCAD by 2-octynoyl-CoA. The time-dependent loss in enzyme activity (expressed in percentage) upon incubation with 2-octynoyl-CoA, for the wild-type and mutant enzymes, is shown. The incubation mixture either contained 279 nM wild-type enzyme and 100 μM 2-octynoyl-CoA or contained 11.6 μM E376D mutant enzyme and 109.5 μM 2-octynoyl-CoA. At different time intervals, a 10 μL aliquot of the incubation mixture was transferred to the reaction mixture containing 100 μM IPCoA, 250 μM $FcPF_6$ in standard phosphate buffer. The initial rate of the enzyme reaction was measured by monitoring the increase in absorption at 367 nm, due to conversion of IPCoA to IACoA. The solid smooth lines are the best fit of the experimental data by the single-exponential rate equation (with offset), with rate constants of 0.031 $\pm$ 0.0002 and 0.002 $\pm$ 0.0002 s^{-1} for the wild-type and E376D mutant enzymes, respectively.

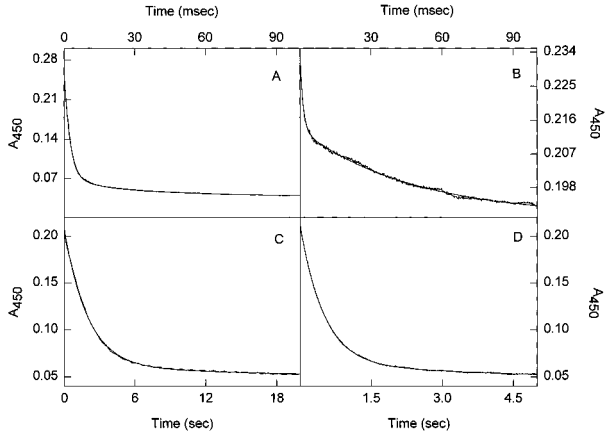

FIGURE 3: Transient kinetics for the octanoyl-CoA-dependent reductive half-reaction of the wild-type and E376D mutant enzymes. The reaction temperature for the data in panels A through C was 5 °C, and that for panel D was 25 °C. Whereas panel A involved the wild-type enzyme, panels B through D involved the E376D mutant enzyme. The concentrations of the enzyme (wild-type or mutant) and octanoyl-CoA in the individual syringes (before mixing concentrations) were 30 μM and 300 μM, respectively. The solid smooth lines are the best fit of the experimental data according to the biphasic rate equation, with the following fast ($1/\tau_{fast}$) and slow ($1/\tau_{slow}$) relaxation rate constants and their corresponding amplitudes (ΔA_{fast} and ΔA_{slow}). Panel A: $1/\tau_{fast} = 398.4 \pm 29.6$, $1/\tau_{slow} = 32.4 \pm 1$ s^{-1}, $\Delta A_{fast} = 0.19 \pm 0.001$, $\Delta A_{slow} = 0.03 \pm 0.009$. Panel B: $1/\tau_{fast} = 810 \pm 26.5$ s^{-1}, $1/\tau_{slow} = 23.5 \pm 0.4$ s^{-1}. $\Delta A_{fast} = 0.021 \pm 0.001$, $\Delta A_{slow} = 0.016 \pm 0.0001$. Panel C: $1/\tau_{fast} = 0.502 \pm 0.001$, $1/\tau_{slow} = 0.048 \pm 0.003$ s^{-1}, $\Delta A_{fast} = 0.147 \pm 0.0003$, $\Delta A_{slow} = 0.013 \pm 0.0003$. Panel D: $1/\tau_{fast} = 2.01 \pm 0.007$, $1/\tau_{slow} = 0.18 \pm 0.03$ s^{-1}, $\Delta A_{fast} = 0.148 \pm 0.001$, $\Delta A_{slow} = 0.019 \pm 0.001$.

These data clearly suggest that the E376D mutation impairs the ability of 2-octynoyl-CoA to inactivate the mutant enzyme by about 16-fold. Such a decrease is presumably due to diminution in the rate of proton transfer from the γ-carbon atom of 2-octynoyl-CoA to the carboxyl group of Asp-376 in the case of the mutant enzyme.

Transient Kinetics for the Wild-Type and E376D Mutant Enzymes. To dissect the specific influence of the E376D mutation on the octanoyl-CoA-dependent reaction of the enzyme, we investigated the transient kinetics for the reductive half-reaction, oxidative half-reaction, dissociation off-rate of the reaction product (octenoyl-CoA) from the oxidized enzyme site, and the interaction of octenoyl-CoA with the wild-type and mutant enzymes.

Reductive Half-Reaction. We compared the transient courses of the octanoyl-CoA-dependent reductive half-reaction utilizing both the wild-type and E376D mutant enzymes. During these experiments 30 μM either wild-type or mutant enzyme was mixed with 300 μM octanoyl-CoA at 5 °C via the stopped-flow syringes, and the time-dependent decrease in absorption changes was recorded at 450 nm. As noted previously (*5*, *15*, *37*), the octanoyl-CoA-dependent reductive half-reaction of the wild-type enzyme (under the above experimental condition) was found to conform to a biphasic reaction profile (Figure 3A), with fast and slow relaxation rate constants of 399 $\pm$ 4 and 32.4 $\pm$ 1 s^{-1}, and their corresponding amplitudes (ΔA_{450}) of 0.19 $\pm$ 0.001 and 0.03 $\pm$ 0.009, respectively. On the other hand, the above reaction involving the E376D mutant enzyme (under an identical experimental condition) yielded a complex reaction profile. The overall reaction was found to be consistent with at least four reaction phases. Since these reaction phases were completed at different times, they were discerned by recording the reaction traces at two different time regimes. Figure 3B shows the stopped-flow trace (at 450 nm) upon mixing 30 μM E376D mutant enzyme with 300 μM octanoyl-CoA at 5 °C for a time period of 100 ms. The solid, smooth line is the best fit of the experimental data for a biphasic kinetic equation, with fast and slow relaxation rate constants of 810 $\pm$ 26.5 and 23.5 $\pm$ 0.4 s^{-1}, and the corresponding amplitudes (ΔA_{450}) of 0.021 $\pm$ 0.0006 and 0.016 $\pm$ 0.00006, respectively. It should be noted that although these fast and slow rate constants of the mutant enzyme are comparable to the corresponding rate constants of the wild-type enzyme (Figure 3; also see *5*, *29*), the amplitude of the fast phase in the case of the wild-type enzyme is about 9-fold higher than that of the mutant enzyme. The mechanistic basis of this discrepancy is elaborated in the Discussion.

Figure 3C shows the stopped-flow trace for the reaction of the E376D mutant enzyme with octanoyl-CoA on a longer time regime (0−20 s), but precisely under the experimental condition of Figure 3B. The experimental data are once again best fitted by the biphasic rate equation, with fast and slow relaxation rate constants of 0.50 $\pm$ 0.001 and 0.05 $\pm$ 0.003 s^{-1}, and the corresponding amplitudes (ΔA_{450}) of 0.147 $\pm$ 0.0003 and 0.013 $\pm$ 0.0003, respectively. It is noteworthy that the latter fast amplitude represents about 74% of the total absorption changes at 450 nm, which corresponds to about 63% reduction of the enzyme-bound FAD. Hence, this amplitude is primarily contributed by the reduction of the enzyme-bound FAD.

To further verify the complex kinetic pattern for the reaction of the E376D mutant enzyme with octanoyl-CoA,

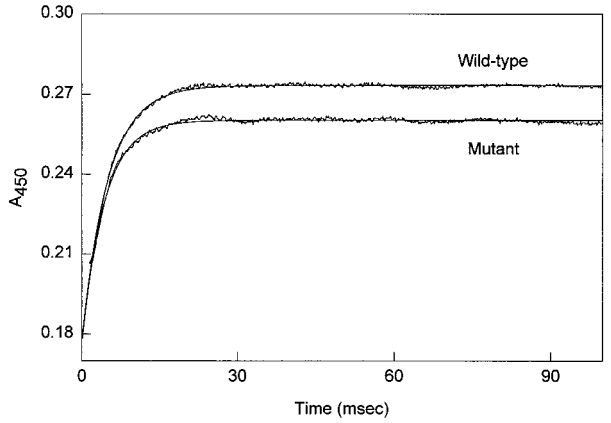

FIGURE 4: Oxidative half-reaction of the wild-type and E376D mutant enzymes. The reaction temperature was 25 °C. The reduced forms of the wild-type and mutant enzymes were produced by mixing 40 μM either wild-type or E376D mutant enzyme with 36 μM octanoyl-CoA via the first two stopped-flow syringes. This was followed by mixing with 1.5 mM $FcPF_6$ via the third stopped-flow syringe, and the time-dependent increase in absorption was monitored at 450 nm. The solid smooth lines are the best fit of the experimental data by the single-exponential rate equation, with rate constants of 196 $\pm$ 0.8 and 214 $\pm$ 1 s^{-1} and the corresponding amplitudes of 0.096 $\pm$ 0.003 and 0.084 $\pm$ 0.005 for the wild-type and E376D mutant enzymes, respectively.

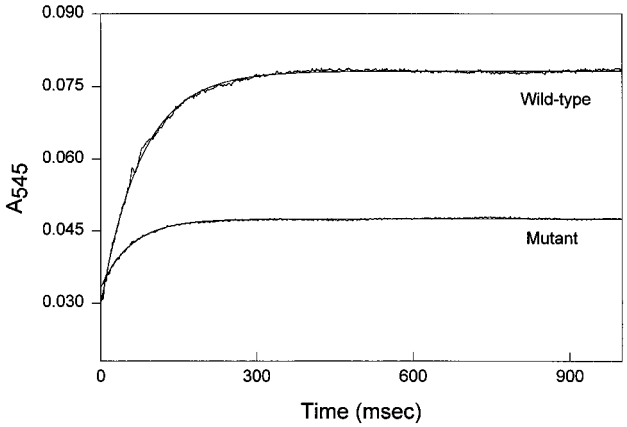

FIGURE 5: Dissociation off-rate of octenoyl-CoA from the oxidized forms of the wild-type and E376D mutant enzymes. The dissociation off-rates were measured by the acetoacetyl-CoA displacement method at 25 °C. In this experiment, 80 μM either wild-type or E376D mutant enzyme was first mixed with 80 μM octenoyl-CoA via the two stopped-flow syringes. The mixture was allowed to age for 2 s, followed by mixing with 2 mM acetoacetyl-CoA via the third stopped-flow syringe. The after mixing concentrations of the enzyme (wild-type or mutant), octenoyl-CoA, and acetoacetyl-CoA were 20 μM, 20 μM, and 1 mM, respectively. The time-dependent increase in absorption was recorded at 545 nm. The solid smooth lines are the best fit of the experimental data by the single-exponential rate equation with rate constants of 12.7 $\pm$ 0.1 and 8.4 $\pm$ 0.1 s^{-1} and the corresponding amplitudes of 0.049 $\pm$ 0.0001 and 0.014 $\pm$ 0.0001 for the wild-type and E376D mutant enzymes, respectively.

we performed the experiment at 25 °C (Figure 3D). At the latter temperature, we could not discern the first two reaction phases (as observed in Figure 3B), due to the rapidity of the reaction at this temperature. However, the control experiment (i.e., the sum of absorption of the mutant enzyme and octanoyl-CoA at 450 nm, without reaction) revealed that an absorption change of 0.029 occurred within the dead time of the stopped-flow system (data not shown). The latter change is similar to the sum of the amplitudes of the fast and slow phases (0.037) of Figure 3B. At 25 °C, the reaction trace on a longer time scale also showed a biphasic kinetic profile, with magnitudes of the fast and slow relaxation rate constants of 2.01 $\pm$ 0.007 and 0.18 $\pm$ 0.03 s^{-1}, respectively. The corresponding amplitudes (ΔA_{450}) of these phases were 0.148 $\pm$ 0.0005 and 0.019 $\pm$ 0.001, suggesting that the reduction of the enzyme-bound FAD occurred during the latter phases.

It should be pointed out that the relaxation rate constant of the third phase at 5 °C (Figure 3C), which corresponds to the fast phase at 25 °C (Figure 3D), is 2.01 s^{-1}, and during this phase about 63% of the enzyme-bound FAD is reduced. Since the relaxation rate constant of 2.01 s^{-1} is qualitatively given by the sum of the forward and reverse rate constants of the fast phase, the former can be approximated to be 1.3 s^{-1}. This rate constant is comparable to the turnover rate of the mutant enzyme (0.75 s^{-1}; Table 1), with octanoyl-CoA as a substrate. The above difference between the two rates is likely to be due to the errors in determination of the k_{cat} and/or approximating the forward rate constant. Hence, it appears likely that the rate-limiting step of the mutant enzyme is primarily conformed by the forward rate constant of the reductive half-reaction. This is further supported by the fact that the rates of the oxidative half-reaction and the dissociation off-rate of octenoyl-CoA are both faster than the turnover rate of the enzyme.

Oxidative Half-Reaction. Figure 4 shows the stopped-flow reaction traces (at 450 nm) for the oxidation of the octanoyl-CoA-reduced wild-type and E376D mutant enzymes by $FcPF_6$. During these experiments, 40 μM enzyme was first mixed with 36 μM octanoyl-CoA via the first two stopped-flow syringes, and the reaction mixture was allowed to age until the enzyme-bound FAD was completely reduced, followed by mixing with 1500 μM $FcPF_6$ via the third stopped-flow syringe (*12*, *29*). Note a marked similarity between the reaction traces of the wild-type and the mutant enzymes. Both these reaction traces are fitted by the single-exponential rate law with rate constants of 196 $\pm$ 0.8 and 213 $\pm$ 1 s^{-1} and their corresponding amplitudes (ΔA_{450}) of 0.096 $\pm$ 0.003 and 0.084 $\pm$ 0.005 for the wild-type and mutant enzymes, respectively. A small difference in the amplitude between the wild-type and mutant enzymes is due to the difference in the extent of FAD reduction by octanoyl-CoA. It should be noted that unlike the reductive half-reaction, the E376D mutation exhibits no influence on the oxidative half-reaction of the enzyme. Furthermore, rate constants of the oxidative half-reaction are much higher than the corresponding turnover rates (see Table 1) of the wild-type and mutant enzymes, respectively, and thus the oxidative half-reaction does not limit the overall rate of either the wild-type or the E376D mutant enzyme.

Dissociation Off-Rate of the Reaction Product. We compared the rate constants for the dissociation (off-rate) of octenoyl-CoA from the oxidized forms of the wild-type and E376D mutant enzymes. As described previously (*15*, *23*), such measurements were performed via the sequential mixing stopped-flow technique, utilizing a high and excessive concentration of acetoacetyl-CoA as a competitive ligand of octenoyl-CoA. Figure 5 shows the stopped-flow traces (at 545 nm) upon mixing 80 μM enzyme (wild-type or mutant) and 90 μM octenoyl-CoA via the first two stopped-flow syringes; the mixture was allowed to age for 2 s, and then

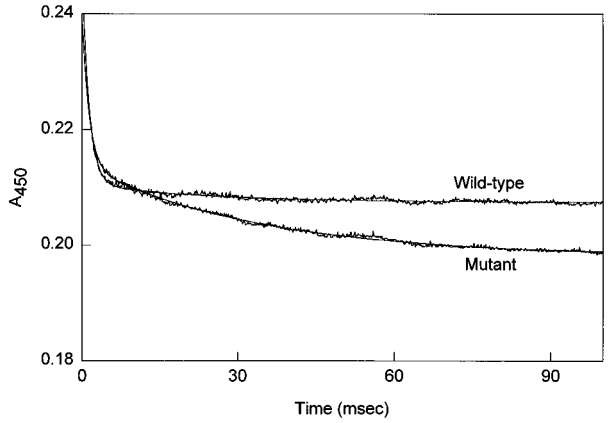

FIGURE 6: Interaction of octenoyl-CoA with the wild-type and E376D mutant enzymes. The time courses for the decrease in absorption at 442 nm were measured upon mixing either 30 μM wild-type or E376D mutant enzyme with 300 μM 2-octenoyl-CoA via the stopped-flow syringes at 5 °C. The solid smooth lines are the best fit of the experimental data according to the double-exponential rate equation with fast and slow relaxation rate constants of 884 ± 16.3 and 79.1 ± 4 s^{-1} for the wild-type and 1000 ± 31 and 32.8 ± 0.3 s^{-1} for the E376D mutant enzyme, respectively. The corresponding amplitudes for the fast and slow phases in the case of the wild-type enzyme were 0.051 ± 0.001 and 0.004 ± 0.0002, respectively, and those in the case of the E376D mutant enzyme were 0.031 ± 0.001 and 0.016 ± 0.0001, respectively.

mixed with 2 mM acetoacetyl-CoA via the third stopped-flow syringe. The after mixing concentrations of enzyme, octenoyl-CoA, and acetoacetyl-CoA were 20 μM, 20 μM, and 1 mM, respectively. The experimental data are consistent with a single-exponential rate equation with rate constants of 12.7 ± 0.1 and 8.4 ± 0.1 s^{-1} and their corresponding amplitudes of 0.049 ± 0.0001 and 0.014 ± 0.0001 for the wild-type and mutant enzymes, respectively. It should be pointed out that the higher amplitude of the reaction trace in the case of the wild-type vis-à-vis the mutant enzyme is due to a higher $\Delta\epsilon_{545}$ in the case of the wild-type enzyme−acetoacetyl-CoA complex as compared to the mutant enzyme−acetoacetyl-CoA complex. It should be further noted that although the dissociation off-rate of octenoyl-CoA from the wild-type enzyme site is comparable to its turnover rate, the dissociation off-rate of octenoyl-CoA from the mutant enzyme is considerably faster than the turnover rate of the mutant enzyme. Hence, unlike the wild-type enzyme, the rate-limiting step of the mutant enzyme is not given by the dissociation off-rate of the reaction product, octenoyl-CoA.

Transient Kinetics for the Interaction of Octenoyl-CoA. As elaborated in the introduction, one of the most interesting aspects of MCAD (both from pig kidney and from human liver) is the marked similarity between the transient kinetic profiles of the octanoyl-CoA-dependent reduction of E−FAD and the binding of octenoyl-CoA to E−FAD (*5, 15*). Since the E376D mutation markedly perturbs the transient kinetic profiles for the reduction of E−FAD by octanoyl-CoA (see above and Figure 3), it was of interest to examine whether the above mutation also influenced the kinetic profile for the binding of octenoyl-CoA to E−FAD. Figure 6 shows the time courses of absorption changes at 442 nm (the wavelength at which the binding of octenoyl-CoA to the enzyme yields the most pronounced absorption changes) upon mixing 30 μM wild-type or mutant enzyme with 300 μM octenoyl-CoA via the stopped-flow syringes. The solid smooth lines are the best fit of the experimental data for the fast and slow relaxation rate constants of 884 ± 16.3 and 79.1 ± 4.0 s^{-1} for the wild-type, and 1000 ± 31 and 32.8 ± 0.3 s^{-1} for the mutant enzyme, respectively. The corresponding fast and slow amplitudes (ΔA_{442}) for the wild-type enzyme were 0.051 ± 0.008 and 0.004 ± 0.0002, respectively, and those for the mutant enzymes were 0.031 ± 0.01 and 0.016 ± 0.0002, respectively. On the basis of these data, it appears that although the Glu376→Asp mutation does not result in significant changes in the fast phase of the enzyme + octenoyl-CoA interaction process, it decreases the rate constant of the slow phase and increases its amplitude. Since the relaxation rate constants are given by the sum of both forward and reverse steps, the above difference is presumably due to a favorable equilibrium distribution between the (E−FAD−octenoyl-CoA)* and (E−FAD−octenoyl-CoA)** species to the latter (see eq 2). Such a difference may arise due to a small change in the protein conformation upon Glu376→Asp mutation. However, a comparative account of the enzyme + octanoyl-CoA reaction and enzyme + octenoyl-CoA binding involving the mutant enzyme exhibits significant differences. As will be elaborated in the Discussion, such differences are due to uncoupling between the proton transfer and protein conformational change steps.

DISCUSSION

The experimental data presented in the previous section provide the following consequences of excision of a methylene group from the side chain of Glu-376 (Glu376→Asp mutation) in the medium chain acyl-CoA dehydrogenase catalyzed reaction. (I) The turnover rates of both IPCoA- and octanoyl-CoA-dependent reactions are impaired by about 20-fold, and there is no selective solvent deuterium isotope effect on the steady-state turnover of the enzyme utilizing the above substrates (Table 1). (II) The rate of inactivation of the enzyme by 2-octynoyl-CoA is impaired by about 16-fold (Figure 2). (III) The transient kinetic profiles as well as their associated rate constants for the octanoyl-CoA-dependent reductive half-reaction of the enzyme are drastically altered (Figure 3). (IV) The rate-limiting step of the octanoyl-CoA-dependent reaction of the enzyme is shifted from the product dissociation step to the forward rate constant of the reductive half-reaction. (V) The intrinsic similarity between the microscopic pathways of the octanoyl-CoA-dependent reductive half-reaction and the enzyme−octenoyl-CoA interaction is abolished (Figures 3 and 6).

The fact that the Glu376→Asp mutation impairs the turnover rates of the IPCoA- and octanoyl-CoA-dependent reactions of MCAD clearly attest to the importance of the Glu-376 residue at the active site of the enzyme during catalysis. The above mutation also impairs the rate of inactivation of the enzyme by 2-octynoyl-CoA (which is known to proceed via abstraction of the γ-proton; see the introduction). An interesting feature of all these reactions is that their corresponding rate constants are decreased by a common magnitude, i.e., by 15−20-fold, due to excision of a methylene group from the side chain of Glu-376. The question arises as to what is the mechanistic basis of such a commonality. This is particularly important since the turnover rates of the IPCoA- and octanoyl-CoA-dependent reactions are limited by different microscopic steps. Whereas

the turnover rate of the IPCoA-dependent reaction is limited by the forward rate constant of the reductive half-reaction, the turnover rate of the octanoyl-CoA-dependent reaction is limited by the dissociation "off-rate" of the reaction product, octenoyl-CoA (*12*, *13*, *29*, *33*). On accounting for the influence of the E376D mutation on the (forward) rate of the reductive half-reaction, it is apparent that the octanoyl-CoA-dependent reduction of the enzyme-bound FAD is decelerated by about 800-fold (see Figure 3). The latter effect is comparable to that obtained upon mutation of Glu165→Asp during the triosephosphate isomerase catalyzed reaction (*17*). On the contrary, the Glu376→Asp mutation decelerates the forward rate of the IPCoA-dependent reductive half-reaction (which is equal to the turnover rate of the enzyme) only by a factor of 20 (see Table 1). Considering that the above effects are mediated via the reduction in the corresponding proton-transfer steps (from the α-carbon of the CoA derivatives to the carboxyl group of Asp-376), it follows that the Glu376→Asp mutation is energetically more costly for octanoyl-CoA (since the reductive half-reaction is decelerated by 800-fold) than for the IPCoA-dependent (where the reductive half-reaction is decelerated only by 20-fold) reaction. The energetic cost of the above mutation during the 2-octynoyl-CoA-dependent inactivation (which is impaired by 16-fold) of the enzyme is comparable to that of the IPCoA-dependent reaction. Given these, it appears that the rate of proton transfer upon Glu376→Asp mutation is affected by different magnitudes involving different CoA derivatives. This is presumably due to the spatial relationship of the proton donor (viz., α-proton in the case of octanoyl-CoA and IPCoA, and γ-proton in the case of 2-octynoyl-CoA) and acceptor (viz., carboxyl group of Glu376 or Asp376) groups in the ground and transition states of the enzyme. Hence, the noted similarity in the diminution in the turnover or inactivation rate constants due to Glu376→Asp mutation is merely due to a coincidence.

The question arises whether the "void" created by excision of a methylene group due to Glu376→Asp mutation is replaced by a water molecule (leaving the conformation of the entire protein molecule unchanged), and such a water molecule mediates the proton transfer reaction between the α-carbon of acyl-CoAs and the carboxyl group of Asp-376. Although a definitive answer to this question must await a high-resolution X-ray crystallographic structure of the E376D mutant enzyme, we believe, if such a water molecule is present between the carboxyl group of Asp-376 and the α-carbon atom of acyl-CoAs, it does not serve as an efficient proton shuttle (i.e., a "general" base) during the enzyme catalysis. This is clearly supported by the fact that the turnover rates of both IPCoA- and octanoyl-CoA-dependent reactions are minimally affected upon substitution of solvent H_2O by D_2O. Given that the ratio of $k_{cat}(H_2O)$ to $k_{cat}(D_2O)$ varies only between 1.5 and 2 for both IPCoA- and octanoyl-CoA-dependent reactions, it is suggestive of the fact that the above effects are nonspecific solvent deuterium isotope effects.

The major effect of the Glu376→Asp mutation is seen on the kinetic profiles as well as the intrinsic rate constants of the octanoyl-CoA-dependent reductive half-reaction of the enzyme (Figure 3). The transient kinetic profile of the latter reaction is changed from biphasic in the case of the wild-type enzyme to tetraphasic upon Glu376→Asp mutation. Although the rate constants of the first two phases of the mutant enzyme are similar to those of the wild-type enzyme, their amplitudes are considerably lower. These amplitudes are comparable to those obtained for the interaction of octenoyl-CoA with the enzyme. Since the absorption changes during the enzyme−octenoyl-CoA interaction are due to changes in the electronic structure of the enzyme-bound FAD, which occurs in concomitant with the changes in the protein conformation (*5*, *15*, *16*), it appears evident that the first two phases during the reductive half-reaction of the mutant enzyme are due to the protein conformational changes. The third phase in the case of the mutant enzyme accompanies a major (about 63%) reduction of the enzyme-bound flavin. This phase and the last (fourth) phase in the case of the mutant enzyme arise due to impairment of the proton-transfer step during the reductive half-reaction. These phases are not present either during the reductive half-reaction of the wild-type enzyme or during the enzyme−octenoyl-CoA interaction. In light of these facts, it appears that in the case of the wild-type enzyme, the fast and slow reaction phases are comprised of both the changes in the electronic structure of the enzyme-bound FAD (with changes in the protein conformation) and the reduction of the enzyme-bound FAD to $FADH_2$. Hence, in the case of the wild-type enzyme, the protein conformational changes are coupled to the reduction of the enzyme bound FAD, and such a coupling is clearly lost upon Glu376→Asp mutation. We are currently investigating the consequences of Glu376→Asp mutation on the structural features of MCAD, and we will report on these findings subsequently.

REFERENCES

1. Bross, P., Engst, S., Strauss, A. W., Kelly, D. P., Rasched, I., and Ghisla, S. (1990) *J. Biol. Chem.* 265, 7116−7119.
2. Lee, H.-J. K., Wang, M., Paschke, R., Nandy, A., Ghisla, S., and Kim, J.-J. P. (1996) *Biochemistry* 35, 12412−12420.
3. Nandy, A., Kieweg, V., Krautle, F.-G., Vock, P., Kuchler, B., Bross, P., Kim, J.-J. P., Rasched, I., and Ghisla, S. (1996) *Biochemistry* 35, 12402−12411.
4. Kiweg, V., Krautle, F.-G., Nandy, A., Engst, S., Vock, P., Abdel-Ghany, A.-G., Bross, P., Gregersen, N., Rasched, I., Strauss, A., Ghisla, G. (1997) *Eur. J. Biochem.* 246, 548−556.
5. Peterson, K. L., Sergienko, E. E., Wu, Y., Kumar, N. R., Strauss, A. W., Oleson, A. E., Muhonen, W. W., Shabb, J. B., and Srivastava, D. K. (1995) *Biochemistry* 34, 14942−14953.
6. Engel, P. C. (1990) in *Chemistry and Biochemistry of Flavoenzymes* (Muller, F., Ed.) Vol. 3, pp 597−655, CRC Press, Boca Raton, FL.
7. Kim, J.-J. P., Wang, M., and Paschke, R. (1993) *Proc. Natl. Acad. Sci. U.S.A.* 90, 7523−7527.
8. Mancini-S, G. J., Stankovich, M. T., Vock, P., Kieweg, V., and Ghisla, S. (1996) in *Flavins and Flavoproteins* (Stevenson, K. J., Massey, V., and Williams, C. H., Jr., Eds.) pp 637−640, University of Calgary Press, Calgary.
9. Ghisla, S., Engst, S., Moll, M., Bross, P., Strauss, A. W., and Kim, J.-J. P. (1992) in *New Developments in Fatty Acid Oxidation* (Coates, P. M., and Tanaka, K., Eds.) pp 127−142, Wiley-Liss, New York.
10. Ghisla, S., Thorpe, C., and Massey, V. (1984) *Biochemistry* 23, 3154−3161.
11. Powell, P. J., and Thorpe, C. (1988) *Biochemistry* 27, 8022−8028.
12. Kumar, N. R., Peterson, K. L., and Srivastava, D. K. (1996) in *Flavins and Flavoproteins* (Stevenson, K. J., Massey, V.,

and Williams, C. W., Eds.), pp 633−636, University of Calgary Press, Calgary.
13. Peterson, K. L., Gu W., and Srivastava, D. K. (1996) in *Flavins and Flavoproteins* (Stevenson, K. J., Massey, V., and Williams, C. W., Eds.), pp 641−644, University of Calgary Press, Calgary.
14. Srivastava, D. K., Johnson, J. K., Kumar, N. R., and Peterson, K. L. (1996) in *Flavins and Flavoproteins* (Stevenson, K. J., Massey, V., and Williams, C. W., Eds.), pp 605−614, University of Calgary Press, Calgary.
15. Kumar, N. R., and Srivastava, D. K. (1994) *Biochemistry 33*, 8833−8841.
16. Kumar, N. R., and Srivastava, D. K. (1995) *Biochemistry 34*, 9434−9443.
17. Raines, R. T., Sutton, E. L., Straus, D. R., Gilbert, W., and Knowles, J. R. (1986) *Biochemistry 25*, 7142−7154.
18. Loll, P. L., and Lattman, E. E. (1990) *Biochemistry 29*, 6866−6873.
19. Nishikawa, S., Morioka, H., Fuchimura, K., Tanaka, T., Uesugi, S., Ohtsuka, E., and Ikehara, M. (1986) *Biochem. Biophys. Res. Commun. 138*, 789−794.
20. Bernert, J. T., and Sprecher, H. (1977) *J. Biol. Chem. 252*, 6737−6744.
21. Freund, K., Mizzner, J., Dick, W., and Thorpe, C. (1985) *Biochemistry 24*, 5996−6002.
22. Lehman, T. C., Hale, D. E., Bhala, A., and Thorpe, C. (1990) *Anal. Biochem.* 186, 280−284.
23. Johnson, J. K., Wang, Z. X., and Srivastava, D. K. (1992) *Biochemistry 31*, 10564−10575.
24. Thorpe, C., Matthews, R. G., and Williams, C. W., Jr. (1979) *Biochemistry 18*, 331−337.
25. Brackett, J. C., Sims, H. F., Steiner, R. D., Nunge, M., Zimmerman, E. M., deMartinville, B., Rinaldo, P., Slaugh, R., and Strauss, A. W. (1994) *J. Clin. Invest. 94*, 1477−1483.
26. Higuchi, R. B., Krummel, B., and Saiki, R. K. (1988) *Nucleic Acids Res. 16*, 7351−7367.
27. Moore, D. D. (1994) *Current Protocols in Molecular Biology* (Ausubel, F. B., Brent, R., Kingston, R. E., Moore, D. D., Seidman, J. G., Smith, J. A., and Struhl, K., Eds.) John Wiley and Sons: Inc., New York.
28. Sambrook, J., Fritsch, E., and Maniatis, T. (1989) in *Molecular cloning: A Laboratory manual*, 2nd ed., Cold Spring Harbor Laboratory, Cold Spring Harbor, NY.
29. Peterson, K. L., and Srivastava, D. K. (1997) *Biochem. J. 325*, 751−760.
30. Weber, K., and Osborn, M. (1969) *J. Biol. Chem. 244*, 4406−4412.
31. Williamson, G., Engel, P. C., Mizzner, J. P., Thorpe, C., and Massey, V. (1982) *J. Biol. Chem. 257*, 4314−4320.
32. Tiffany, K. A., Roberts, D. R., Wang, M., Paschke, R., Mohsen, A.-W., A., Vockley, J., and Kim, J.-J. P. (1997) *Biochemistry 36*, 8455−8464.
33. Johnson, J. K., and Srivastava, D. K. (1993) *Biochemistry 32*, 8004−8013.
34. Johnson, J. K., Kumar, N. R., and Srivastava, D. K. (1993) *Biochemistry 32*, 11575−11585.
35. Johnson, J. K., Kumar, N. R., and Srivastava, D. K. (1994) *Biochemistry 33*, 4738−4744.
36. Srivastava, D. K., Kumar, N. R., and Peterson, K. L. (1995) *Biochemistry 34*, 4625−4632.
37. Hall, C. L., Lambeth, J. D., and Kamin, H., (1979) *J. Biol. Chem. 254*, 2023−2031.
38. Rauno, G., Brash, D. E., and Kidd, K. K. (1991) in *PCR: The first few cycles. Perkin-Elmer Cetus Amplifications 7*, 1−4.
39. Schowen, B., and Schowen, R. L. (1982) *Methods Enzymol. 87*, 551−606.

BI972590S